

Gradual Domain Adaptation for Graph Learning

Pui Ieng Lei, Ximing Chen, Yijun Sheng, Yanyan Liu, Jingzhi Guo, and Zhiguo Gong

Abstract—Existing literature lacks a graph domain adaptation technique for handling large distribution shifts, primarily due to the difficulty in simulating an evolving path from source to target graph. To make a breakthrough, we present a *graph gradual domain adaptation* (GGDA) framework with the construction of a compact domain sequence that minimizes information loss in adaptations. Our approach starts with an efficient generation of knowledge-preserving intermediate graphs over the Fused Gromov-Wasserstein (FGW) metric. A GGDA domain sequence is then constructed upon the bridging data pool via a novel vertex-based domain progression, which comprises “close” vertex selections and adaptive domain advancement to enhance inter-domain transferability. Theoretically, our framework concretizes the intractable inter-domain Wasserstein distance via implementable upper and lower bounds, enabling flexible adjustments of this metric for optimizing domain formation. Extensive experiments under various transfer scenarios validate the superior performance of our GGDA framework.

Index Terms—Graphs and networks, data mining, neural nets

I. INTRODUCTION

Domain adaptation (DA) is a powerful solution for transferring knowledge from a label-rich (i.e., source) domain to a relevant but label-scarce (i.e., target) domain under data distribution shifts [1]. In general, most existing DA algorithms are developed under an assumption that data samples within each domain are independent and identically distributed (IID) [2]–[9]. Recently, this assumption has encountered challenges due to the explosive increase of non-IID data in the real world (e.g., social networks, traffic networks, etc.). This, along with the rapid development of graph neural networks (GNNs) [10]–[13], urges the study of DA on graph-structured data [14]–[20].

In a graph DA problem, the source and target graphs are each viewed as a collection of not only the data objects (i.e., nodes) but also their relations (i.e., edges). Therefore, unlike IID learning, a data representation in graph DA should encode information from both the data object and its related objects. Accordingly, a typical graph DA framework is to learn a graph encoder that captures data dependency via neighborhood aggregations and, in the meantime, aligns the source and target distributions in a latent space to enable knowledge transfer on a domain-invariant basis [14], [18], [21]–[23]. However,

theoretical analysis has shown that domain-invariant techniques perform poorly under a large discrepancy in marginal distributions due to information distortion [24]. This issue is further exacerbated in non-IID scenarios, where data attributes and relations may shift jointly. Motivated by this, our paper delves into the critical challenge of graph domain adaptation under larger shifts. Specifically, we follow an unsupervised domain adaptation (UDA) setting, where the target domain is fully unlabeled.

In the case of IID-based UDA, to handle larger shifts, several algorithms integrate the use of unlabeled intermediate domains between source and target domains [25]–[29]. Specifically, a line of research investigates *gradual domain adaptation* (GDA), which leverages iterative model adaptations over a sequence of intermediate domains shifting from source to target [30]–[35]. Essentially, GDA turns a UDA problem with a large domain gap into several sub-UDA problems with small domain gaps, thereby bounding the generalization error of transfer. While the sequence of intermediate data is sometimes available from data collection, e.g., portraits taken across years (IID) or evolving social networks (non-IID), in many cases, it is hard or even impossible to find suitable intermediate data. To address this issue, in IID scenarios, approaches such as interpolations and adversarial training have been employed to generate virtual intermediate data [28], [29], [31], [35].

Despite its promising performance, the GDA algorithm has only been examined in an IID setting, while its applicability to non-IID data is still under-explored due to the high intricacy involved. However, given the growing ubiquity of graph-structured data in the real world, it is critical that the performance of graph DA models does not plummet under larger shifts, and this is precisely where GDA can play a valuable role. Motivated by this, in this paper, we explore a new *graph gradual domain adaptation* (GGDA) framework from theoretical and empirical perspectives. Assuming no intermediate data is initially available, the central question here is: *In a non-IID context of graph-structured data, how should the intermediate domain sequence be constructed to ensure a high target accuracy from GGDA?*

To answer this question, we first identify two key criteria: (1) the intermediate domains should be constructed to *minimize information loss* upon GGDA, and (2) the construction scheme should allow *flexible adjustments* of the inter-domain Wasserstein distance, $W_p(\mu_t, \mu_{t+1})$, to enable a search for the optimal domain formation. In a graph context, primary challenges are twofold: (1) $W_p(\mu_t, \mu_{t+1})$ is inherently implicit as there is no explicitly defined structure space to accommodate all possible instance relations, and (2) the generation of every instance must account for both itself and neighbors.

Based on these considerations, we propose a novel GGDA framework as follows. We first develop an efficient technique

Pui Ieng Lei is with the Faculty of Science and Technology, University of Macau, Macau, China. Email: yc37460@um.edu.mo.

Ximing Chen is with the Faculty of Science and Technology, University of Macau, Macau, China. Email: yc37921@um.edu.mo.

Yijun Sheng is with the Faculty of Science and Technology, University of Macau, Macau, China. Email: yc17419@um.edu.mo.

Yanyan Liu is with the Faculty of Science and Technology, University of Macau, Macau, China. Email: yc07402@um.edu.mo.

Jingzhi Guo is with the Faculty of Science and Technology, University of Macau, Macau, China. Email: jzguo@um.edu.mo.

Zhiguo Gong is with the Faculty of Science and Technology, University of Macau, Macau, China. Email: fstzgg@um.edu.mo.

This work has been submitted to the IEEE for possible publication. Copyright may be transferred without notice, after which this version may no longer be accessible.

to generate a sequence of intermediate graphs with weighted Fréchet mean over the Fused Gromov-Wasserstein (FGW) metric [36], a graph distance metric defined as the minimal cost of transporting both features and structures between two graphs. In this way, we avoid knowing the implicit cross-domain structures. Our proposed entropy-guided matching, combined with coupling constraints in FGW computations, maximizes the infusion of valid knowledge from the given data into the generated data. Upon the generated data bridge, we introduce a novel domain progression scheme that constructs GGDA domains with enhanced inter-domain compactness for robust transfers. The scheme consists of two modules: regularized vertex selection for constructing a subsequent domain and adaptive mass decay for removing obsolete nodes from the current domain. By traversing the generated graphs and forming each domain with "close" vertices, the resulting cross-domain adaptation effectively preserves transferable and discriminative knowledge.

Theoretically, we demonstrate that the intractable $W_p(\mu_t, \mu_{t+1})$ is now concretized by its lower bound from the FGW metric and its upper bound from our vertex selection regularization. Moreover, a hyperparameter governing the scale of vertex selection under our prioritization enables flexible adjustments of $W_p(\mu_t, \mu_{t+1})$ to optimize the solution without repetitive data generation. Here is a summary of our contributions:

- To the best of our knowledge, we are the first to investigate *gradual domain adaptation on graphs* and propose a solution tailored to *large domain gaps* in graph DA tasks.
- Our GGDA framework constructs a compact domain sequence for stable inter-graph knowledge transfer. Specifically, we tackle the non-trivial issue of structure implicitness by designing tractable modules with theoretical bounding effects.
- Extensive experiments on fifteen datasets validate our theoretical insights and the effectiveness of the proposed framework. In particular, our framework beats the best baseline by an average of +5.02%.

II. RELATED WORKS

This section provides a concise overview of prior research relevant to our study. A comprehensive discussion of related works can be found in the appendix.

A. Graph Domain Adaptation

A widely adopted framework for node-level graph domain adaptation is to perform adversarial training and learn domain-invariant representations that fool the domain discriminator [14]–[22], [37]–[43]. Beyond adversarial methods, alternative strategies have been explored, such as ego-graph information maximization [44], spectral regularization that modulates the GNN Lipschitz constant for error bounding [23], and generation of new source graph [45]. Despite these advances, none of the existing approaches have addressed the critical scenario of large distribution gaps between source and target graphs. Graph-level domain adaptation, on the other hand, focuses on graph classifications and treats each graph as an individual sample, resembling traditional IID settings [46], [47].

B. Intermediate Domains for IID Domain Adaptation

The use of intermediate domains has shown promise in addressing IID domain adaptation tasks [25]–[33], [35], [48]–[50]. For the generation of intermediate domains, some earlier works construct them as generative subspaces on a specific (e.g., Grassmann) manifold [48], [49], while later works generate them on a sample level to better integrate with deep learning techniques [28], [29], [31], [35], [51]. Gradual domain adaptation (GDA) is a line of research where the source model is gradually shifted towards the target domain along a path formed by the intermediate domain sequence, either retrieved from data or generated via linear interpolation and mixup strategies [30]–[35], [52]. Nevertheless, the effect of both intermediate domains and GDA for non-IID graph domain adaptation remains unexplored.

III. PRELIMINARIES

This section establishes our formal setting, including: (1) key mathematical notations, (2) definitions of graph space and domain distributions, and (3) specification of models and learning objectives in GGDA.

A. Notations

A simplex of n bins is denoted by $\Sigma_n = \{h \in \mathbb{R}_+^n \mid \sum_i h_i = 1\}$. For two histograms $h \in \Sigma_n$ and $h' \in \Sigma_m$, we denote the set of all couplings between h and h' by $\Pi(h, h') = \{\pi \in \mathbb{R}_+^{n \times m} \mid \sum_i \pi_{i,j} = h'_j; \sum_j \pi_{i,j} = h_i\}$. For a space Ω and $x \in \Omega$, δ_x denotes the Dirac measure in x . The support of probability measure $\mu \in P(\Omega)$ is denoted by $\text{supp}(\mu) = \text{argmin}_A \{|A| \mid A \subset \Omega; \mu(\Omega \setminus A) = 0\}$.

B. Graph Space

In this paper, a graph is viewed as a distribution sampled from a product space of features, structures, and classes. An undirected attributed graph $\mathcal{G} = (\mathcal{V}, \mathcal{E})$ contains the set of vertices \mathcal{V} and edges \mathcal{E} . Each vertex $v_i \in \mathcal{V}$ has (1) a feature representation x_i in space (Ω_x, d_x) , (2) a structure representation a_i in space (Ω_a, C) , and (3) a class label y_i in space (Ω_y, d_y) .

Specifically, the feature space Ω_x is a Euclidean space, with d_x being the Euclidean distance. For simplicity, we focus on binary classification in this paper, with node labels $y_i \in \{-1, 1\}$ and $\Omega_y := \mathbb{R}$. The structure space Ω_a is an implicit space, upon which the exact positions of nodes are not observed, and $C : \Omega_a \times \Omega_a \rightarrow \mathbb{R}_+$ measures the distance between pairs of nodes reflected by their structures in the graph, such as node adjacency or shortest path distance. Note that in graph DA setting, since relational semantics persist across domains (e.g., for citation networks from different time periods, edges always represent citation relationships), we assume a shared ground structure space (Ω_a, C) for all graphs. In other words, the structural distance between nodes from different graphs is well-defined by C , even if the corresponding inter-graph edges (e.g., potential citations between papers from different time periods) are unobserved.

For a graph with n vertices, a histogram $h \in \Sigma_n$ describes each vertex's relative importance within the graph (e.g., uniform or degree distribution). This allows the graph to be represented as $\mu = \sum_{i=1}^n h_i \delta_{(x_i, a_i, y_i)}$, a fully supported probability measure over the product space $\Omega_x \times \Omega_a \times \Omega_y$. Given that not all labels are observed, the graph can also be represented in a reduced product space $\Omega_x \times \Omega_a$, i.e., $\mu = \sum_{i=1}^n h_i \delta_{(x_i, a_i)}$.

In a graph domain adaptation setting, we view all graphs concerned to be drawn from a shared space $\Omega_x \times \Omega_a \times \Omega_y$, but with shifted probability distributions.

C. Models and Objectives

Consider a node classification task, where the goal is to predict node labels given node features and graph topology. Given a model family Θ , for each $\theta \in \Theta$, a model $M_\theta : \Omega_x \times \Omega_a \rightarrow \Omega_y$ outputs the classification predictions. Each model can be viewed as a composite function with respect to some Euclidean embedding space (Ω_z, d_z) , i.e., $M_\theta = \Psi_\theta \circ \Phi_\theta$, where $\Phi_\theta : \Omega_x \times \Omega_a \rightarrow \Omega_z$ (graph encoder) and $\Psi_\theta : \Omega_z \rightarrow \Omega_y$ (classifier).

Consider $T + 1$ graph distributions (i.e., domains), denoted by $\mu_0, \mu_1, \dots, \mu_T$. For unsupervised graph DA, $\mu_0 = \mu_S$ is a fully-labeled source domain and μ_T is a fully-unlabeled target domain. For GGDA, μ_1, \dots, μ_{T-1} are unknown intermediate domains transitioning from source to target. The population loss in t -th domain is defined as

$$\epsilon_t(\theta) \equiv \epsilon_{\mu_t}(\theta) = \mathbb{E}_{x,a,y \sim \mu_t} [\ell(M_\theta(x, a), y)], \quad (1)$$

where ℓ is the loss function. The goal is to find a model M_θ that yields a low classification error on the target graph, i.e., low $\epsilon_T(\theta)$.

IV. ASSUMPTIONS

Our framework builds upon the following assumptions, further details of which are provided in the appendix.

Assumption 1 (Covariate shift) Assume the conditional distribution $p(y|x, a)$ is invariant over the ground space [53].

Assumption 2 (Metrics on product spaces) Assume the metric on $(\Omega_x \times \Omega_a, d_{(x,a)})$ is a linear combination of the metrics on the respective space, i.e., $d_{(x,a)}((x, a), (x', a')) = (1 - \alpha)d_x(x, x') + \alpha C(a, a')$ for some $\alpha \in [0, 1]$. Meanwhile, assume the metric on $(\Omega_x \times \Omega_a \times \Omega_y, d_{(x,a,y)})$ is the Manhattan distance along the input and output coordinates, i.e., $\Omega_x \times \Omega_a$ and Ω_y .

Assumption 3 (Bounded model complexity) Given a graph domain where the number of training samples is n and the maximum degree is d_{max} , assume the Rademacher complexity of the considered GNN model family Φ is bounded as [54]:

$$\mathfrak{R}_n(\Phi) \leq \mathcal{O}\left(\frac{d_{max}}{\sqrt{n}}\right). \quad (2)$$

Assumption 4 (Lipschitz model) Assume for any $\theta \in \Theta$, the model M_θ is R -Lipschitz in the input space $\Omega_x \times \Omega_a$, and the model Ψ_θ is \tilde{R} -Lipschitz in the embedding space Ω_z .

Assumption 5 (Lipschitz loss) Assume the loss function ℓ is ρ -Lipschitz in the output space Ω_y .

V. ANALYSIS OF GGDA DOMAIN GENERATION

Our goal is to transfer knowledge between the relevant source and target graphs under a large distribution shift. While no intermediate data is available, we aim to generate intermediate domains appropriately to promote a stable long-range knowledge transfer. All proofs for this paper can be found in the appendix.

The first important consideration is the criteria that intermediate domains should satisfy such that the target error from GGDA on the domain sequence is well-bounded. Following previous GDA work [33], we adopt an online learning perspective and obtain the following generalization bound for graph-based gradual domain adaptation:

$$\epsilon_T(\theta_T) \leq \epsilon_0(\theta_0) + \mathcal{O}\left(T\Delta + T\left(e + \sqrt{\frac{\log(1/\delta')}{b}}\right)\right) + \tilde{\mathcal{O}}\left(\frac{1}{\sqrt{nT}}\right),$$

$$\text{where } \Delta = \frac{1}{T} \sum_{t=0}^{T-1} W_p(\mu_t, \mu_{t+1}) \text{ and } \mu_t = \sum_{i=1}^{n_t} h_i^t \delta_{(x_i^t, a_i^t, y_i^t)}. \quad (3)$$

Here n indicates the average number of vertices in each domain. Both the terms e and $\sqrt{\frac{\log(1/\delta')}{b}}$ quantify the inherent non-IID nature of the given dataset and fall outside our scope of consideration. Our analysis centers on the measure Δ , defined as the average p-Wasserstein distance (i.e., W_p) between consecutive domains, which reflects the difference in features, structures, and classes between cross-domain samples under optimal coupling. We observe an inverse relationship between the optimal Δ and T [33], suggesting that when the average distance between consecutive domains is large, the number of intermediate domains should be fewer, and vice versa. Note that this does not imply that the bound is tightest at $T = 1$ (i.e., non-GDA). In fact, based on Eq. (3) as well as past empirical GDA studies [30], [33], the optimal performance is typically achieved at a "sweet spot" when T is moderately large (i.e., Δ is moderately small). This further underscores the need for a GDA algorithm on graphs to divide a large shift into multiple smaller shifts for enhancing adaptation performance.

Given the above analysis, we conclude two criteria that the intermediate domain generation should satisfy for a successful GGDA: (1) the length of the path connecting source and target, i.e., $T\Delta$, should be small in order to curb the transfer information loss; and (2) a search for the optimal Δ should be conducted under an inverse relationship between Δ and T . To fulfill these criteria, there are three main challenges as follows:

- 1) Both criteria necessitate domain generation according to inter-domain distance $W_p(\mu_t, \mu_{t+1})$ over $\Omega_x \times \Omega_a \times \Omega_y$. This is non-trivial since (i) $W_p(\mu_t, \mu_{t+1})$ over Ω_a is inherently implicit, and (ii) during generation, each created sample (i.e., vertex) within domain μ should be characterized not only by its own information but also by that of its neighbors.
- 2) For criterion (1), an ideal solution is to generate a Wasserstein geodesic over $\Omega_x \times \Omega_a \times \Omega_y$, yet this is extremely challenging in practice due to the intractable optimization for an exact Wasserstein geodesic of attributed topological data.

3) While the p-Wasserstein metric is defined on $\Omega_x \times \Omega_a \times \Omega_y$, only the source domain is labeled. How the intermediate domains should be generated to effectively integrate class information (i.e., y -dimension) poses another key challenge.

To tackle challenge (1), we propose to facilitate domain generation through concretization of graph metric (especially over the implicit topology on Ω_a) by leveraging the FGW distance as a bridge between abstract distance W_p and practical implementations. Regarding challenge (2), we refine the concept of Wasserstein geodesic into a practical realization in this setting: *minimizing information loss during the GGDA process*. Specifically, we aim to approximate the shortest path between source and target with intermediate domains that minimize information loss upon model adaptations. This is achieved by a combination of FGW optimizations and a subsequent vertex selection process for domain constructions. Additionally, the regularized vertex selection addresses challenge (3) via enhanced pseudo-labeling for domain progression. In the following sections, we will provide the detailed explanations accordingly.

VI. GRAPH GENERATION OVER FGW METRIC

While we wish to generate intermediate domains that adhere to the distance defined in Eq. (3), a primary challenge is that $W_p(\mu_t, \mu_{t+1})$ over the product space $\Omega_x \times \Omega_a \times \Omega_y$ is intractable, as the metric for measuring the structural distance between cross-graph samples over Ω_a is implicit (i.e., no inter-graph edges). This presents a dilemma specific to a non-IID context, where each sample is characterized not only by itself but also by its relationships with other attributed samples. To bridge the gap between theoretical insights and practical implementations, we require a well-defined and tractable inter-graph distribution distance that considers both features and structures. To this end, we adopt the Fused Gromov-Wasserstein (FGW) distance defined as follows.

Definition 1 (FGW distance) Let two attributed graphs be $\mu = \sum_{i=1}^n h_i \delta_{(x_i, a_i)}$ and $\nu = \sum_{j=1}^m h'_j \delta_{(x'_j, a'_j)}$. Let $d_x(i, j) = d_x(x_i, x'_j)$ be the distance between cross-network features, while $C(i, k) = C(a_i, a_k)$ and $C'(j, l) = C(a'_j, a'_l)$ are the respective structure matrix for μ and ν . Given the set of all admissible couplings $\Pi(h, h')$ and $\alpha \in [0, 1]$, the FGW distance in the discrete case is defined as [36]

$$FGW_{\alpha, p, q}(\mu, \nu) = \left(\min_{\pi \in \Pi(h, h')} E_{\alpha, p, q}(\pi) \right)^{\frac{1}{p}}, \quad \text{where}$$

$$E_{\alpha, p, q}(\pi) = \sum_{i, j, k, l} \left[(1 - \alpha) d_x(i, j)^q + \alpha |C(i, k) - C'(j, l)|^q \right]^p \pi_{i, j} \pi_{k, l}. \quad (4)$$

$E(\pi)$ is the cost of transporting between graphs with node matching strategy π , which includes the costs of transporting features across single nodes and transporting structures across pairs of nodes. The FGW distance is the minimal cost given by the optimal coupling. Hence, the computation of FGW is built upon sample coupling that preserves both feature and relation similarities. Under such constraints, node i is matched to node

j only if they have similar features and their neighbors (i.e., k, l) also present a correspondence.

A. Fast Entropy-Guided Graph Generation

Having defined an implementable graph metric, we now proceed to generate the intermediate graphs for bridging the gap between source and target graphs. Note that at this stage, "intermediate graphs" do not yet refer to "intermediate domains". We propose to generate a sequence of $K - 1$ intermediate graphs $\{\tilde{\mu}_k\}_{k=1}^{K-1}$ via the weighted Fréchet mean [55] over the FGW metric on $\Omega_x \times \Omega_a$ (without Ω_y as μ_T is unlabeled). However, directly computing the Fréchet mean between the *entire* source and target graphs can be costly, especially in the case of large graphs. To enhance both efficiency and knowledge preservation, we introduce a partition-based, entropy-guided graph generation strategy, where each intermediate graph $\tilde{\mu}_k$ is generated as a combination of smaller graphs $\{\tilde{\mu}_{k_i}\}_i$.

To begin with, we transform the source and target graphs into P_S and P_T partitions with METIS [56], an algorithm that minimizes the number of cross-partition edges. Then, the overall idea is to generate each $\tilde{\mu}_{k_i}$ using a pair of source and target partitions, denoted by $\hat{\mu}_{m(P_t)}^S$ and $\hat{\mu}_{P_t}^T$, with indices $m(P_t) \in \{1, 2, \dots, P_S\}$ and $P_t \in \{1, 2, \dots, P_T\}$. The function $m(\cdot)$ represents an index matching between source and target partitions, which we aim to optimize to enhance knowledge preservation during graph generation.

To achieve this, we first initiate a warm-up phase to obtain a preliminary matching $\hat{m}(\cdot)$ before graph generation. Let $m(\cdot)$ be a random matching, $n_{m(P_t)}^S$ and $n_{P_t}^T$ be the size of the partition pair, $Y_{m(P_t), c}^S \in \{0, 1\}^{n_{m(P_t)}^S}$ be an indicator of source nodes belonging to class $c \in \{-1, 1\}$, and $\pi^*(m(P_t), P_t) \in [0, 1]^{n_{m(P_t)}^S \times n_{P_t}^T}$ be the normalized FGW optimal coupling on $\Omega_x \times \Omega_a$ between the partition pair. Then, for each $P_t \in \{1, 2, \dots, P_T\}$, we compute the following:

$$f_{(m(P_t), P_t), c} = \left[\text{diag}(Y_{m(P_t), c}^S) \cdot \pi^*(m(P_t), P_t) \right]^T \cdot \mathbf{1},$$

$$F_{(m(P_t), P_t)} = \left[f_{(m(P_t), P_t), -1}, f_{(m(P_t), P_t), 1} \right],$$

$$H_{(m(P_t), P_t)} = \frac{1}{n_{P_t}^T} \sum_{i=1}^{n_{P_t}^T} \left[- \sum_j F_{(m(P_t), P_t), ij} \cdot \log F_{(m(P_t), P_t), ij} \right]. \quad (5)$$

Here $F_{(m(P_t), P_t)} \in [0, 1]^{n_{P_t}^T \times 2}$ contains each target node's push-forward class distribution, and $H_{(m(P_t), P_t)} \in \mathbb{R}$ is the average target node class entropy. While such class distribution is only an estimation, it is a useful indicator of information compatibility between the pair $(m(P_t), P_t)$, i.e., a large H indicates that much valid class information has been lost by coupling this pair over FGW. Combining the effects of source class entropy H^S and FGW distance, for each pair $(m(P_t), P_t)$, we derive a measure of information loss

$$S_{\text{loss}}(m(P_t), P_t) = \left(H_{(m(P_t), P_t)} / H_{m(P_t)}^S \right) \cdot FGW(\hat{\mu}_{m(P_t)}^S, \hat{\mu}_{P_t}^T), \quad (6)$$

where all components are normalized. During the warm-up phase, different initializations of $m(\cdot) \in \mathcal{M}(\cdot)$ are employed, and a preliminary matching is set to $\hat{m}(P_t) = \operatorname{argmin}_{m(P_t) \in \mathcal{M}(P_t)} S_{loss}(m(P_t), P_t)$.

We now proceed to knowledge-preserving graph generation with matched partition pairs. In this phase, $m(P_t)$ is set to $\hat{m}(P_t)$ with a probability $\propto 1/S_{loss}(\hat{m}(P_t), P_t)$ and is set to a new matching otherwise. With this matching strategy, we generate a sequence of unlabeled intermediate graphs $\{\tilde{\mu}_k\}_{k=1}^{K-1}$ over $\Omega_x \times \Omega_a$ via the following weighted Fréchet mean optimization for each k :

$$\begin{aligned} \tilde{\mu}_k &= \frac{1}{\Gamma} \sum_i \tilde{\mu}_{k_i}, \quad \text{where} \\ \tilde{\mu}_{k_i} &= \operatorname{argmin}_{\mu} \left[\left(\frac{K-k}{K} \right) \cdot FGW(\mu, \hat{\mu}_{m(P_{t,i})}^S) \right. \\ &\quad \left. + \left(\frac{k}{K} \right) \cdot FGW(\mu, \hat{\mu}_{P_{t,i}}^T) \right], \end{aligned} \quad (7)$$

with $P_{t,i} \sim \text{Uniform}\{1, 2, \dots, P_T\}$ and Γ being a normalizing factor. This scheme constructs a bridging graph sequence $\{\tilde{\mu}_k\}_{k=1}^{K-1}$ by incrementally shifting the position of $\tilde{\mu}_k$ between μ_S and μ_T over the FGW metric. Meanwhile, the index matching $\hat{m}(\cdot)$ is continuously refined whenever a new matching yields a smaller S_{loss} than the previous one. In this phase, $S_{loss}(m(P_t), P_t)$ is computed by substituting (1) the source-intermediate optimal coupling $\pi^*(m(P_{t,i}), k_i)$ in Eq. (5) and (2) the distance sum $FGW(\hat{\mu}_{m(P_{t,i})}^S, \tilde{\mu}_{k_i}) + FGW(\tilde{\mu}_{k_i}, \hat{\mu}_{P_{t,i}}^T)$ in Eq. (6), both obtained directly from Fréchet mean optimization, i.e., no extra computations. Since the entropy reflecting information loss is now evaluated on $\tilde{\mu}_{k_i}$, the information integrity within the generated intermediate graphs can be further boosted. Overall, with our accelerated module, the time complexity of graph generation largely reduces from $\mathcal{O}(n^3)$ to $\mathcal{O}(Pn_p^3)$, where P is the average number of partitions and n_p is the average partition size (see complexity analysis).

B. Analysis: Why Is FGW-Based Graph Generation Important for a Successful GGDA?

While the FGW-generated graphs do not inherently conform to $W_p(\mu_t, \mu_{t+1})$ over $\Omega_x \times \Omega_a \times \Omega_y$ in Eq. (3), this proposed generation process is central to our algorithm for two reasons.

First, the minimization in Eq. (7) serves as a mechanism of information preservation in the construction of intermediate graphs by aiming to reduce the FGW distance between $\tilde{\mu}_{k_i}$ and $\hat{\mu}_S/\hat{\mu}_T$. The sample correspondence constraint inherent in FGW optimization drives the ego-graphs distributed in the generated $\tilde{\mu}_k$ to preserve and interpolate the characteristics of source and target ego-graphs. In other words, this approach serves to *minimize the information loss* over $\Omega_x \times \Omega_a$ when generating the bridging data sequence.

Second, as discussed in Section V, the domain generation should be conducted by searching for an optimal $W_p(\mu_t, \mu_{t+1})$ over $\Omega_x \times \Omega_a \times \Omega_y$. While this W_p distance is intractable, it is, in fact, lower bounded by the FGW distance over $\Omega_x \times \Omega_a$, as shown below.

Proposition 2 For graph measures $\mu(x, a, y) = \sum_{i=1}^n h_i \delta_{(x_i, a_i, y_i)}$ and $\nu(x', a', y') = \sum_{j=1}^m h'_j \delta_{(x'_j, a'_j, y'_j)}$,

along with their marginal measures $\mu(x, a) = \sum_{i=1}^n h_i \delta_{(x_i, a_i)}$ and $\nu(x', a') = \sum_{j=1}^m h'_j \delta_{(x'_j, a'_j)}$,

$$W_p(\mu(x, a, y), \nu(x', a', y')) \geq FGW_{\alpha, p, 1}(\mu(x, a), \nu(x', a'))/2. \quad (8)$$

This relation implies that, in order to generate data with a certain W_p distance, a necessary condition is to reduce the FGW distance between the data. Intuitively, it means that the presence of generated data with a small FGW distance is crucial for establishing a data pool that enables subsequent refinements for achieving the desired $W_p(\mu_t, \mu_{t+1})$ and, ultimately, a successful GGDA process.

VII. DOMAIN CONSTRUCTION AND GGDA

Gradual domain adaptation (GDA) involves model training on a sequence of T domains with labeled data, such that the model shifts from source domain μ_0 to target domain μ_T with small steps over the intermediate domains $\{\mu_t\}_{t=1}^{T-1}$. Specifically, since only the source domain contains ground-truth labels, each intermediate domain is defined with pseudo-labels obtained during iterative training. To perform GDA on graphs, one major consideration, as discussed above, is how to properly define the intermediate domain sequence over $\Omega_x \times \Omega_a \times \Omega_y$ to minimize information loss during the GGDA process. Specifically, it is crucial to ensure that pseudo-labeling can be performed accurately when defining each labeled intermediate domain under our algorithm, such that the label accuracy decay over the entire GGDA process can be well restrained.

A. Analysis: Vertex-Based Domain Construction for GGDA

Given the FGW-generated graph sequence, it might be tempting to define each *intermediate domain* μ_t as a single *intermediate graph* $\tilde{\mu}_{k|k=t}$ with post-assigned pseudo-labels. However, such a definition is not optimal, as the FGW distance itself is not an upper bound of $|\epsilon_{k+1}(\theta) - \epsilon_k(\theta)|$, i.e., it does not inherently ensure information transferability (and thus the correctness of pseudo-labeling) from $\tilde{\mu}_k$ to $\tilde{\mu}_{k+1}$. To this end, we propose to construct each domain μ_t progressively along the training by selecting vertices from the data pool. This method offers two key advantages as described below.

First, the final task of GGDA is vertex-based (i.e., node classification), focusing on the characteristics of each vertex encoded in its ego-graph. Therefore, rather than directly using a complete FGW-generated graph as an individual domain, defining each subsequent domain as a set of vertices selected based on their encoded knowledge relative to vertices from the previous domain better preserves the transferable and discriminative knowledge during adaptation. As presented in Figure 1, assume we start with the labeled domain $\mu_S = \mu_0$ for the training. Since vertices within the graph sequence inherently possess different relevance to μ_0 in terms of the $d_{(x, a, y)}$ metric (i.e., distance over $\Omega_x \times \Omega_a \times \Omega_y$), if we manage to select vertices close to μ_0 (marked with "+") from the data sequence for constructing the subsequent domain μ_1 , the resulting cross-domain knowledge transfer can be enhanced by minimal information loss.

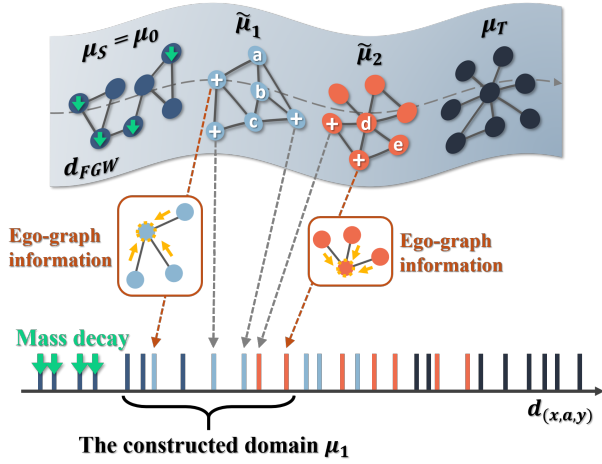


Fig. 1. Illustration highlighting the rationale of our GGDA framework. The upper part shows the generated graph sequence over FGW metric, and the lower part shows the corresponding vertex relations over product space distance $d_{(x,a,y)}$. μ_0 (in dark blue) is initially labeled. "+" indicates added vertices and green lower arrow indicates downweighted vertices.

Second, since the newly constructed domain can contain vertices from different graphs, the domain's connections to unused vertices in the pool are naturally maintained through existing edges. Knowledge propagation upon these edges improves the correctness of pseudo-labeling on linked vertices and, thus, the quality of the next constructed domain. Put differently, the existence of inter-domain edges is the key to a successful GGDA as it signifies a higher domain transfer potential and a smaller information loss between consecutive domains. In Figure 1, consider vertices marked with "+" being correctly pseudo-labeled and included in domain μ_1 . In this case, vertices a to e , as prospective components of domain μ_2 , can be assigned accurate pseudo-labels by gathering reliable messages directly from their labeled neighbors. Such an insight regarding inter-domain connectivity can also be stated from a theoretical perspective, as illustrated in the following proposition.

Proposition 3 Consider graph domains $\mu = \sum_{i=1}^n h_i \delta_{(x_i, a_i, y_i)}$ and $\nu = \sum_{j=1}^m h'_j \delta_{(x'_j, a'_j, y'_j)}$ with uniform weights h and h' . Let \mathcal{E} be the set of unit-weight edges linking μ and ν and $\tilde{\pi}$ be an arbitrary coupling satisfying $\tilde{\pi}_{i,j} = \frac{1}{nm} \mathbb{1}_{\{(i,j) \in \mathcal{E}\}}$. For any $\theta \in \Theta$, the population loss on μ and ν given by M_θ satisfies

$$|\epsilon_\mu(\theta) - \epsilon_\nu(\theta)| \leq \rho(\zeta_1 + \zeta_2), \quad \text{where}$$

$$\zeta_1 = \frac{\sqrt{R^2 + 1}}{n \cdot m} \sum_{(i,j) \in \mathcal{E}} \left(\|z_i(\theta) - z'_j(\theta)\| + |y_i - y'_j| \right),$$

$$\zeta_2 = \sqrt{R^2 + 1} \cdot \left[\min_{\tilde{\pi}} \left(\sum_{(i,j) \notin \mathcal{E}} d_{(x,a,y)} \left((x_i, a_i, y_i), (x'_j, a'_j, y'_j) \right)^p \cdot \tilde{\pi}_{i,j} \right) \right]^{\frac{1}{p}}. \quad (9)$$

When transferring a model between arbitrary graph domains μ and ν , the error bound consists of two components (i.e., ζ_1 and ζ_2) regarding node pairs *with* and *without* inter-domain edges. For ζ_1 , $\sum_{(i,j) \in \mathcal{E}} \|z_i(\theta) - z'_j(\theta)\|$ is small as most GNNs

act as a graph Laplacian regularization that constrains the learned embeddings of two connected nodes to be similar [57]. Meanwhile, $\sum_{(i,j) \in \mathcal{E}} |y_i - y'_j|$ is small if the graphs are homophilic. For ζ_2 , however, the distance $\sum_{(i,j) \notin \mathcal{E}} d_{(x,a,y)}^p$ can be unbounded. We therefore expect a tighter bound when consecutive domains are not mutually isolated.

B. The Domain Progression Framework

Motivated by the analysis, we propose a GGDA framework with the domain sequence $\{\mu_t\}_{t=0}^T$ constructed progressively in a vertex-based manner along the training. Specifically, given the current domain, we define the subsequent domain with two novel modules: regularized vertex selection and adaptive mass decay.

Let $|M_\theta(x, a)|$ be the geometric margin and $\text{sign}(M_\theta(x, a))$ be the prediction, respectively. Further, we consider the entire generated graph sequence as a single batched graph μ_B over $\Omega_x \times \Omega_a$, where $\mathcal{V}_B := \text{supp}(\mu_B) = \bigcup_{k=1}^{K-1} \text{supp}(\tilde{\mu}_k) \cup \text{supp}(\mu_S) \cup \text{supp}(\mu_T)$, and we initialize a mass decay mask $w_{v_b}^0 = 1$ for all $v_b \in \mathcal{V}_B$. At first, only nodes from the source graph are labeled, so we define $\mu_0 = \mu_S = \sum_{i=1}^{n_S} h_i^S \delta_{(x_i^S, a_i^S, y_i^S)}$ with $h_i^S = 1/n_S$. In each upcoming iteration, we perform the two modules below to construct the subsequent domain μ_{t+1} and shift the model from μ_t to μ_{t+1} .¹

1) *Vertex Selection for Constructing Next Domain:* Let $\mathcal{V}_t^t := \text{supp}(\mu_t)$ denote the set of vertices of the current domain μ_t and $\mathcal{V}_u^t := \mathcal{V}_B \setminus (\bigcup_{t'=0}^t \mathcal{V}_t^{t'})$ be the set of unused vertices within the data sequence. First, we train a new model θ_t on the current domain μ_t with loss $\mathbb{E}_{x,a,\hat{y} \sim \mu_t} [\ell(M_{\theta_t}(x, a), \hat{y})] = \sum_{v_l \in \mathcal{V}_l^t} h_l^t \cdot \ell(M_{\theta_t}(x_l, a_l), \hat{y}_l)$, where \hat{y} is either a pseudo-label or a ground-truth label. In the inference phase, for each $v_u \in \mathcal{V}_u^t$, compute the regularized score

$$c_u^t = |M_{\theta_t}(x_u, a_u)| \cdot \exp\left(-\frac{d_u^t}{\max_{\{v_{u'} \in \mathcal{V}_u^t\}} d_{u'}^t} \cdot \eta\right), \quad (10)$$

where $d_u^t = \min_{v_l \in \mathcal{V}_l^t} d_z(\Phi_{\theta_t}(x_u, a_u), \Phi_{\theta_t}(x_l, a_l))$.

Here d_z is the Euclidean distance. In this module, we first obtain the node embeddings by aggregating the feature and structure information of each vertex encoded in its ego-graph, which is either given or generated over the FGW metric. Then, an η -penalty mechanism prioritizes vertices with high classification confidence within the embedding neighborhood of μ_t . Specifically, vertices are sorted by c_u^t and selected within a constraint κ , ratio of the number of new pseudo-labels per class to the number of source labels per class. The selected vertex set, denoted by \mathcal{V}_{pl}^t , will be included in the next domain μ_{t+1} with pseudo-labels $\hat{y}_{pl} = \text{sign}(M_{\theta_t}(x_{pl}, a_{pl}))$ for $v_{pl} \in \mathcal{V}_{pl}^t$. Note that sharpened pseudo-labels (i.e., -1 or 1), rather than probabilities, are assigned to encourage the update of model parameters [30]. To illustrate the rationale behind this module, we present the following proposition.

Proposition 4 Let $\Phi_{\tilde{\theta}} : \Omega_x \times \Omega_a \rightarrow \Omega_z$ be an (L, γ) -quasiisometric graph embedding [58]. Let $\mu(z|\tilde{\theta}) =$

¹From here till the end of section VII-B, we denote $(x_{v_*}, a_{v_*}, \hat{y}_{v_*}, h_{v_*}, w_{v_*})$ by $(x_*, a_*, \hat{y}_*, h_*, w_*)$.

$\sum_{i=1}^n h_i \delta_{z_i|\tilde{\theta}}, \nu(z'|\tilde{\theta}) = \sum_{j=1}^m h'_j \delta_{z'_j|\tilde{\theta}}$, and $\pi^* = \operatorname{argmin}_{\pi \in \Pi(h, h')} \sum_{i,j} d_z(z_i|\tilde{\theta}, z'_j|\tilde{\theta})^p \pi_{i,j}$. Then we have

$$\begin{aligned}
 W_p(\mu(x, a, y), \nu(x', a', y')) &\leq \xi \text{ and } |\epsilon_\mu(\theta) - \epsilon_\nu(\theta)| \cdot \mathcal{O}(\rho^{-1}) \leq \xi, \\
 \text{where } \xi &= L \left[W_\infty(\mu(z|\tilde{\theta}), \nu(z'|\tilde{\theta})) + \gamma \right. \\
 &\quad \left. + \frac{1}{L} \left(\sum_{i,j} |y_i - y'_j|^p \pi_{i,j}^* \right)^{\frac{1}{p}} \right]. \tag{11}
 \end{aligned}$$

From Proposition 4, two conclusions in relation to our approach can be drawn: (1) Under the covariate shift assumption, our vertex selection strategy based on the sorted score c_u^t adheres to ξ formulation by prioritizing samples that are within the Ω_z neighborhood and distant from the decision boundary. Therefore, modifying κ , which controls the scale of class-unbiased vertex selection under c_u^t -prioritization, enables flexible adjustment of $W_p(\mu_t, \mu_{t+1})$ over $\Omega_x \times \Omega_a \times \Omega_y$ via its upper bound ξ while satisfying an inverse relationship between Δ and T , i.e., realization of an efficient global search for optimal GGDA domain path formation without requiring any repetitive data generation. (2) Meanwhile, since our proposed prioritization favors the selection of vertices close to μ_t over the metric $d_{(x,a,y)}$ for inclusion in the next domain μ_{t+1} , it ensures *minimal information loss* by largely preserving transferrable and discriminative knowledge from μ_t to μ_{t+1} . Accordingly, a bounding effect on the local generalization error $|\epsilon_{t+1}(\theta) - \epsilon_t(\theta)|$ can be established.

2) *Adaptive Mass Decay of Vertices*: Given the stochasticity in \mathcal{V}_{pl}^t , strictly excluding all vertices \mathcal{V}_i^t from \mathcal{V}_i^{t+1} may result in low inter-domain connectivity in the succeeding iteration, degrading pseudo-label quality. Moreover, since a new model is trained in every domain, significantly more generated data is required if each domain contains only new vertices, which is inefficient. To this end, we propose an adaptive decay on the distribution mass of \mathcal{V}_i^t . Let the set of labeled nodes be $\mathcal{V}_{pll}^t := \mathcal{V}_l^t \cup \mathcal{V}_{pl}^t$. In every iteration, we store the label score $\hat{c}_{pll}^t = \hat{y}_{pll} \cdot M_{\theta_t}(x_{pll}, a_{pll})$ for $v_{pll} \in \mathcal{V}_{pll}^t$. Then, if $t \geq 1$, we compute the mass decay for $v_l \in \mathcal{V}_l^t$ as

$$\lambda_l^t = \exp\left(-\left[1 - \min\left(\frac{\hat{y}_l \cdot M_{\theta_t}(x_l, a_l)}{\hat{c}_l^{t-1}}, 1\right)\right] \cdot \beta\right). \tag{12}$$

This computation identifies the model flow after training in a new domain by quantifying label correctness degradation. Nodes with degraded labels will be downweighted in the next constructed domain to promote model advancement, with β regulating the mass decay level. Accordingly, we update the mask $w_l^t = w_l^{t-1} \cdot \lambda_l^t$ for $v_l \in \mathcal{V}_l^t$ cumulatively and define the next domain distribution as

$$\begin{aligned}
 \mu_{t+1} &= \frac{1}{\Gamma} \left(\sum_{v_l \in \mathcal{V}_l^t} w_l^t \cdot \delta_{(x_l, a_l, \hat{y}_l)} + \sum_{v_{pl} \in \mathcal{V}_{pl}^t} \delta_{(x_{pl}, a_{pl}, \hat{y}_{pl})} \right) \\
 &= \sum_{v_{pll} \in \mathcal{V}_{pll}^t} h_{pll}^{t+1} \cdot \delta_{(x_{pll}, a_{pll}, \hat{y}_{pll})}, \tag{13}
 \end{aligned}$$

where Γ is a normalizing factor such that $\sum h_{pll}^{t+1} = 1$. In practice, we can keep only the top- k weighted samples in $\operatorname{supp}(\mu_{t+1})$ and assign a mass of 0 to others, with k being the

average size of source and target graphs. The decay technique is conceptually illustrated in Figure 1, with a minor distinction that this technique takes effect only when $t \geq 1$ (i.e., starting from the construction of μ_2). Note that while some target vertices might be labeled prior to the final stage, mass decay is not applied to these vertices as our goal is to adapt to the target graph. The GGDA process concludes with one final training when sufficient target vertices are confidently labeled.

VIII. COMPLEXITY ANALYSIS

For the generation of intermediate graphs, let the average number of partitions be P and the average partition size be $n_p \ll \max(n_S, n_T)$. Then, the METIS partitioning takes $\mathcal{O}(Pn_p + (Pn_p)^2 + P \log(P)) = \mathcal{O}((Pn_p)^2)$, the warmup phase takes $\mathcal{O}(Pn_p^3)$, and the weighted Fréchet mean generation takes $\mathcal{O}(KPI n_p^3)$, with I denoting the number of iterations for block coordinate descent (BCD) [55]. Overall, WLOG, the generation phase in GGDA takes $\mathcal{O}(KPI n_p^3)$. Note that if the generation is conducted using the entire source and target graphs without partitioning, the time complexity would escalate to $\mathcal{O}(KIn^3)$, with n being the average size of source and target graphs, resulting in significantly lower efficiency.

For the domain progression framework, the time complexity of model training in each domain is $\mathcal{O}(h|A_t^+|d^2)$, where h is the number of hops for GNN aggregations, d is the latent dimension, and $|A_t^+|$ is the number of edges within the subgraph formed by the set of labeled vertices in the current domain (i.e., $\mathcal{V}_l^t := \operatorname{supp}(\mu_t)$) and their h -hop ego graphs. The time complexity of each subsequent domain construction is $\mathcal{O}(|\mathcal{V}_l^t| |\mathcal{V}_u^t| d^2)$, where $|\mathcal{V}_u^t|$ is the number of samples in the data pool that have not been labeled before.

IX. EXPERIMENTS

Our goal is to examine whether our GGDA framework, with the constructed domain sequence, improves graph knowledge transfer. We focus on cross-network node classifications, where source labels are used for training and target labels are used for validation and testing under a 2:8 ratio [17]. We conduct transfer experiments on fifteen graph datasets. Additional experiments, implementation details, and data statistics are provided in the appendix.

A. Datasets

For datasets within the following four groups, we use one as source and the other as target.

- **ACM** (pre-2008), **Citation** (post-2010), and **DBLP** (2004 to 2008) (denoted by **A**, **C**, **D**): multi-label citation networks extracted from ArnetMiner [21];
- **ACM2** (2000 to 2010) and **DBLP2** (post-2010), (denoted by **A2**, **D2**): another pre-processed version of single-label citation networks [14];
- **Blog1** and **Blog2** (denoted by **B1**, **B2**): social networks from BlogCatalog, with 30% of the binary attributes randomly flipped to enlarge discrepancy [59];
- **Arxiv 2007, 2016, 2018**: Arxiv computer science citation networks partitioned by time (all from year 1950) [60].

TABLE I
MICRO-F1 AND MACRO-F1 SCORES (I.E., F1MI AND F1MA) OF NODE CLASSIFICATIONS ON THE TARGET GRAPH.

	A to C		A to D		C to A		C to D		D to A		D to C		Δ_{Mean}
	F1MI	F1MA											
CDAN	77.4±0.3	74.7±0.5	69.6±0.5	65.3±1.5	73.7±0.3	72.5±0.5	73.9±0.3	70.9±0.6	69.0±0.4	66.3±0.7	74.3±0.3	70.8±0.6	+0.3
MDD	76.4±0.4	72.9±0.7	67.6±0.6	61.2±1.6	74.5±0.5	73.4±0.7	73.2±0.4	70.2±0.5	69.8±0.4	66.6±0.8	74.5±0.5	70.3±0.9	-0.4
UDA-GCN	74.0±0.7	71.2±1.5	69.0±0.8	61.3±2.4	72.6±0.5	71.4±0.6	71.5±0.6	66.0±2.7	70.4±0.7	67.7±2.3	74.5±0.4	71.0±1.1	-1.2
ACDNE	78.9±0.3	77.3±0.3	72.2±0.3	69.9±0.3	76.3±0.1	74.6±0.1	74.3±0.3	72.9±0.3	71.6±0.4	70.5±0.4	79.2±0.2	77.1±0.3	+3.3
ASN	78.6±0.7	73.6±1.9	72.7±1.1	66.7±2.8	72.8±0.8	72.7±1.4	74.5±0.7	72.0±1.2	69.0±1.2	68.5±3.0	78.1±0.3	74.1±1.2	+1.5
GRADE	70.8±0.6	68.4±0.8	66.4±0.4	61.6±2.1	67.9±0.3	66.3±0.4	69.6±0.5	66.3±1.0	65.0±0.7	62.1±1.0	68.3±0.5	65.2±1.2	-4.8
StruRW	65.1±2.4	63.2±1.8	68.0±2.1	62.4±2.4	70.6±2.4	66.3±2.4	71.8±2.0	70.4±1.6	65.6±2.1	61.7±1.5	69.2±2.0	60.7±2.2	-5.0
SpecReg	67.5±1.6	64.3±2.3	66.4±1.4	61.8±2.3	68.7±1.4	65.2±3.1	71.8±1.0	65.9±2.1	65.9±1.5	58.8±3.8	67.0±1.8	58.9±1.7	-6.1
GraphAlign	73.2±1.1	70.1±1.1	67.5±1.4	64.6±1.2	67.2±1.1	66.6±1.1	71.6±1.1	68.2±1.8	59.6±1.6	58.8±1.0	66.0±0.8	62.9±1.7	-4.9
A2GNN	75.5±0.3	77.4±0.3	62.1±0.4	66.3±0.3	76.3±0.2	74.9±0.1	70.5±0.4	73.5±0.3	71.7±0.3	71.5±0.2	77.5±0.2	77.8±0.1	+1.6
Pair-Align	72.4±0.6	68.3±0.6	67.5±0.5	64.3±0.3	71.2±0.7	68.5±0.3	71.3±0.3	70.4±0.2	66.1±0.4	62.9±0.6	72.4±0.5	67.2±0.4	-2.7
TDSS	79.6±0.6	77.4±0.9	74.1±0.5	69.7±0.5	74.3±0.2	75.3±0.3	75.2±0.3	73.2±0.6	71.3±0.8	71.6±0.7	80.2±0.3	77.4±0.9	+3.7
GGDA-GCN	80.3±0.3	78.8±0.2	74.7±0.3	72.2±0.3	76.0±0.1	75.9±0.2	75.7±0.5	74.3±0.5	73.7±0.3	73.2±0.3	81.6±0.3	80.7±0.2	+5.2
GGDA-GAT	81.9±0.2	80.4±0.2	77.2±0.2	74.9±0.4	77.1±0.2	76.6±0.2	77.4±0.3	75.9±0.4	75.8±0.3	75.8±0.3	81.5±0.2	80.3±0.2	+6.6
GGDA-SAGE	78.0±0.3	76.8±0.3	72.4±0.6	70.0±0.5	75.6±0.2	75.6±0.3	74.1±0.5	72.3±0.7	70.8±0.3	71.3±0.4	76.3±0.5	76.0±0.5	+2.8
Oracle	97.3±0.1	96.9±0.1	96.9±0.1	96.8±0.1	97.0±0.1	97.0±0.1	96.9±0.1	96.8±0.1	97.0±0.1	97.0±0.1	97.3±0.1	96.9±0.1	

TABLE II
NODE CLASSIFICATION ACCURACY ON THE TARGET GRAPH. OOM INDICATES OUT-OF-MEMORY ERRORS.

	Arxiv 2007 to					To the last step of shift generation					Δ_{Mean}	
	A2 to D2	D2 to A2	B1 to B2	B2 to B1	Arxiv 2016	Arxiv 2018	Cora	CiteSeer	ENGB	DE		PTBR
CDAN	75.8±1.8	67.5±0.6	48.0±1.0	45.7±0.9	47.4±0.1	42.6±0.4	70.2±4.2	67.8±3.6	68.6±1.9	70.7±1.8	66.5±2.3	+1.1
MDD	74.2±1.5	69.8±1.3	44.0±0.7	43.5±0.8	52.8±0.5	51.3±1.3	59.2±1.7	64.1±3.2	65.6±4.2	67.9±2.2	65.9±0.4	-0.1
UDA-GCN	79.1±2.1	71.5±1.0	43.6±1.8	45.8±2.5	54.1±0.2	53.5±0.6	56.5±3.6	71.4±4.5	62.2±3.4	69.2±2.8	71.6±2.6	+1.8
ACDNE	70.1±1.4	60.3±1.5	53.1±1.3	51.3±1.3	43.5±0.6	40.9±1.3	60.4±3.9	53.6±3.1	50.8±2.7	56.8±2.6	68.1±2.2	-4.5
ASN	85.2±1.2	64.9±1.4	30.1±1.3	38.2±2.3	OOM	OOM	78.8±1.9	70.9±3.0	56.5±1.0	59.6±2.8	67.7±2.7	+1.4
GRADE	61.1±1.9	64.4±2.4	42.5±1.3	41.4±1.0	46.8±0.4	OOM	57.9±3.2	66.5±2.5	58.1±2.8	61.2±3.3	63.4±3.3	-3.6
StruRW	63.7±2.8	66.6±2.7	38.7±2.6	31.9±1.3	31.7±0.7	27.2±0.7	67.6±1.9	62.1±4.3	55.6±2.5	60.8±2.4	61.7±2.5	-8.3
SpecReg	75.6±6.9	68.0±2.0	44.7±1.0	43.7±1.0	53.2±0.5	47.6±1.9	72.0±4.3	75.6±3.7	68.1±3.6	69.7±1.4	69.5±1.2	+2.6
GraphAlign	67.8±1.4	68.0±1.6	45.1±1.2	45.9±0.4	30.1±0.3	27.5±0.7	61.0±2.4	56.2±5.2	69.4±3.8	69.9±4.8	67.8±2.0	-4.6
A2GNN	76.1±0.1	67.9±0.7	37.2±1.6	39.5±1.2	48.4±1.1	40.1±2.6	79.7±1.9	70.4±1.7	67.7±2.2	67.1±2.1	68.9±1.7	+0.4
Pair-Align	63.3±0.4	65.7±0.4	39.1±0.7	34.0±0.6	39.2±0.4	37.2±0.7	60.7±1.4	71.4±2.7	61.5±2.0	60.4±1.3	67.9±1.9	-5.3
TDSS	72.5±0.7	64.2±0.7	34.1±1.1	32.9±0.8	43.3±0.4	OOM	79.7±1.4	70.5±2.2	62.3±1.3	62.0±1.4	69.1±1.5	-0.9
GGDA-GCN	91.5±0.5	70.0±0.8	52.4±1.7	49.3±0.4	56.8±0.5	56.6±0.5	86.6±2.1	74.1±3.4	75.3±0.6	74.6±0.4	72.2±0.8	+9.1
GGDA-GAT	91.5±0.4	70.3±0.5	31.5±0.6	30.9±0.9	54.7±0.4	54.1±0.5	82.6±2.2	82.7±1.1	74.2±1.6	74.5±1.7	76.9±1.5	+5.9
GGDA-SAGE	78.5±0.6	58.2±0.5	50.2±1.0	50.3±1.0	55.0±0.1	53.2±0.4	87.4±1.2	83.6±1.1	61.8±1.2	64.8±1.0	70.5±0.9	+4.0
GGDA-GT	/	/	/	/	/	/	93.8±0.2	88.5±0.2	77.7±0.4	74.8±0.7	77.3±0.3	
Oracle	92.4±0.1	99.2±0.1	71.4±2.2	72.3±0.9	67.5±0.1	67.9±0.1	99.0±0.2	95.0±0.2	81.1±0.4	77.6±0.4	78.0±0.4	

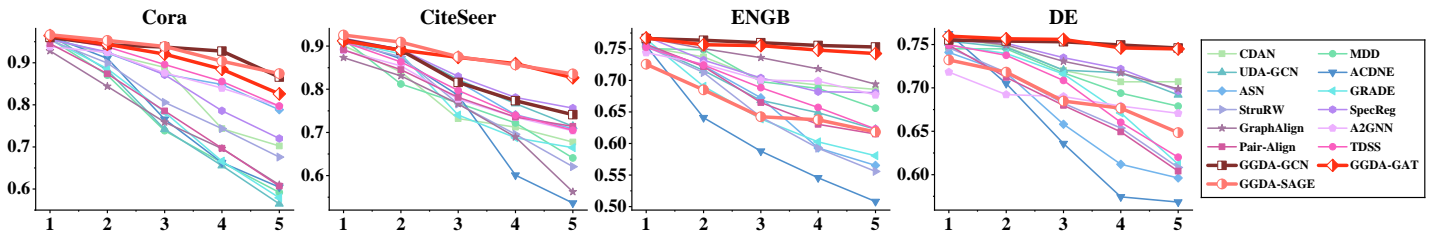


Fig. 2. Node classification accuracy on target graphs with varying levels of discrepancy from the source graph. The x-axis shows the source-target discrepancy level ranked from 1 (closest) to 5 (farthest). The y-axis shows the classification accuracy.

For citation networks **Cora** and **CiteSeer** [61], as well as Twitch social networks **ENGB**, **DE**, and **PTBR** [62], we simulate a *multi-step shifting process* independently on each graph to mimic gradual data shifts. Specifically, we perform

5 steps of class-wise feature shifts generated with Gaussian noise. This effectively shifts the distribution in $\Omega_x \times \Omega_a$ since both $p(x)$ and $p(a|x)$ have changed accordingly. These datasets with multi-step shifting will be used for evaluation in

TABLE III
PERFORMANCE DROP IN TARGET GRAPH NODE CLASSIFICATIONS ACROSS VARIANTS COMPARED TO THE COMPLETE GGDA FRAMEWORK.

	A to D	D to C	C to A	A2 to D2	B1 to B2	Arxiv(07-16)	Arxiv(07-18)	CiteSeer	DE	PTBR	Avg. Drop
Source	-10.7±0.7	-11.0±0.9	-6.0±0.2	-17.0±0.9	-15.1±1.7	-5.6±0.9	-7.8±0.9	-15.8±4.9	-34.9±0.6	-37.2±1.1	-16.1
Direct ST	-6.7±0.6	-5.0±0.5	-3.2±0.3	-11.8±1.2	-11.2±2.4	-5.1±0.8	-7.6±1.1	-7.9±5.0	-7.3±6.4	-22.7±2.9	-8.9
DIR	-9.6±1.3	-13.1±1.2	-8.9±0.8	-11.1±3.5	-4.3±3.4	-4.3±1.0	-4.1±1.1	-21.2±6.5	-3.1±3.8	-6.6±1.4	-8.6
GGDA-I	-2.5±0.7	-5.2±0.6	-1.5±0.4	-7.5±2.6	-10.2±3.1	-2.1±1.0	-2.9±1.1	-4.1±7.1	-6.1±3.7	-4.7±4.1	-4.7
GGDA-R	-2.7±0.7	-1.3±0.7	-1.7±0.6	-0.7±0.6	-3.8±2.1	-2.0±0.5	-2.0±0.9	-2.0±5.9	-0.7±0.7	-1.5±1.0	-1.9

different ways, as detailed later.

B. Baselines

We compare our GGDA framework with the following baselines: **CDAN** [63], **MDD** [64], **UDA-GCN** [14], **ACDNE** [21], **ASN** [15], **GRADE** [18], **StruRW** [17], **SpecReg** [23], **GraphAlign** [45], **A2GNN** [19], **Pair-Align** [43], and **TDSS** [65]. Specifically, CDAN and MDD are non-graph DA methods, for which we replace the encoder with GCN [10]. All other baselines are graph DA methods under the **domain-invariant representation (DIR)** framework, except for GraphAlign, which is the first data-centric graph DA method introduced recently. While multiple baselines incorporate advanced encoder designs to enhance transfer performance, for our **GGDA** framework, we focus on three fundamental encoders in this paper: **GCN**, **GAT**, and **GraphSAGE** [10]–[12]. Additionally, we include two baselines trained with ground-truth information. **GGDA-GT** performs GGDA on the ground-truth intermediate graphs from the *multi-step shifting process*, while **Oracle** is trained on a labeled target graph.

C. Main Results

Table I, Table II and Figure 2 present the performance of graph domain adaptations, with F1 scores for multi-label cases and accuracy scores for single-label cases. Δ_{Mean} in the tables indicates how a model’s performance compares to the mean performance across all models. For the *multi-step shifting* datasets, Table II shows the case where only the graph from the last step of shift generation is used as the target, while Figure 2 shows the case where graphs from each step of shift generation are treated as target graphs with different discrepancies from the source graph.

As shown in the tables, our proposed GGDA framework consistently outperforms other baselines given the intermediate domain construction that aims to minimize information loss upon adaptations and flexibly handles transfer scenarios with varied discrepancies. Moreover, the constructed domains effectively simulate the underlying data flow that bridges the gap, as evidenced by the small difference in target accuracy between our GGDA framework and GGDA-GT, which uses the actual intermediate data from the multi-step shifting process. Meanwhile, Figure 2 illustrates that GGDA-GCN and GGDA-GAT are the least susceptible to an increasing source-target discrepancy, and the high vulnerability of DIR-based models suggests that enforcing an alignment on domain distributions can lead to information distortion and backfire when the domain discrepancy is large. Such a limitation of DIR has also been theoretically validated in previous studies [24].

D. Ablation Studies

To investigate the effectiveness of different components, we conduct ablation studies as follows. (1) **Source**: direct transfer with a classifier trained on source; (2) **Direct ST**: self-training (i.e., iterative pseudo-labeling) without intermediate samples; (3) **DIR**: a prevalent graph DA framework with an adversarial domain classifier for distribution alignment; (4) **GGDA-I (Isolated)**: GGDA with each isolated graph $\tilde{\mu}_k$ as a separate domain; (5) **GGDA-R (Random)**: GGDA with a random matching function $m(\cdot)$ for graph generation. We adopt GCN in all cases, with the results shown in Table III. Particularly, the significant performance drop of Direct ST and DIR highlights the crucial role of intermediate domains in exploiting the underlying data patterns for a robust graph DA. Meanwhile, DIR shows signs of negative transfer (i.e., lower accuracy than Source), underscoring the instability of domain alignment and its heavy reliance on additional model designs. The performance drop of GGDA-I validates the effectiveness of our dual modules in enhancing GGDA via the bonding of knowledge-preserving vertices and adaptive domain advancement, while the performance drop of GGDA-R reflects the improved information integrity from entropy-guided matching in graph generation.

E. Hyperparameter Analysis

The effects of κ and β are shown in Figure 3 and 4. From Figure 3, we observe that adjusting κ enables flexible domain constructions under varying inter-domain distance $W_p(\mu_t, \mu_{t+1})$ while maintaining an inverse relationship between the average distance Δ and the number of domains T . Meanwhile, Figure 4 shows that the optimal GGDA domain path occurs at a “sweet spot” when κ , and thus T , is not too small or too large, which aligns with the initial theoretical analysis. As for β , which governs the pace of weight decay, setting it to 0 equates to self-training on the entire graph sequence without considering distribution shifts, while an overly large β causes rapid information decay before full utilization, both of which can deteriorate transfer performance.

F. Visualization of Target Representation Space

Figure 5 illustrates the final target representation space given by the symbolic DIR model, UDA-GCN, and our proposed GGDA framework. Specifically, we project the node embeddings onto a two-dimensional space via the t-SNE algorithm [66]. In the visualizations, the node embeddings produced by UDA-GCN exhibit greater overlap and mixing between different classes, while the ones generated by GGDA

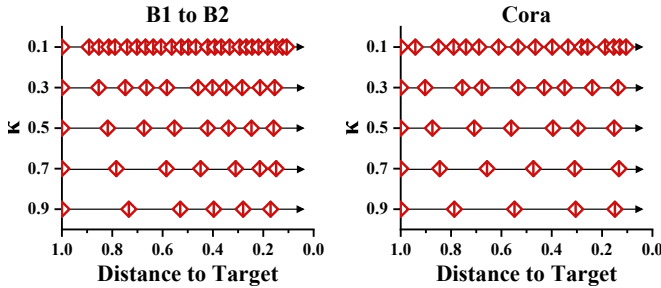


Fig. 3. Progression of the constructed domain sequence under different κ . The x-axis shows the normalized embedding distance between the current and target domains.

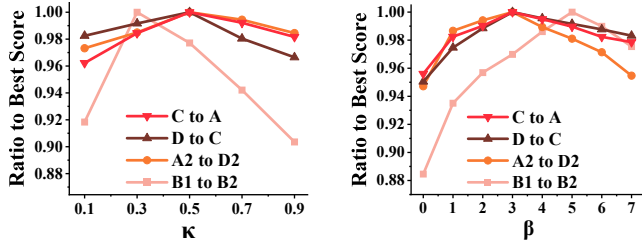


Fig. 4. Performance of our GGDA framework with varying values of hyperparameters κ and β .

demonstrate a well-separated clustering with more pronounced class boundaries. The improved ability of GGDA to learn class-discriminative target representations is attributed to its careful domain sequence constructions that aim for the optimal adaptation path to minimize information loss and reduce irrelevant noise. The preservation of transferable information from the labeled source graph allows GGDA to achieve stable transfer under arbitrary source-target discrepancies.

G. Visualization of Knowledge Transfer in GGDA

To delve into the process of knowledge transfer in GGDA, we conduct an experiment on a synthetic dataset generated using Contextual Stochastic Block Model (CSBM) [67], where node attributes and edges are generated independently given node labels. Specifically, we construct the source and target graphs to each contain 300 nodes, with 100 nodes from each of the 3 classes. We generate the node attributes for the three classes with Gaussians $\mathbb{P}_0 = \mathcal{N}([0, -3], I/2)$, $\mathbb{P}_1 = \mathcal{N}([0, 0], I/2)$, and $\mathbb{P}_2 = \mathcal{N}([0, 3], I/2)$ for the source graph, and Gaussians $\mathbb{P}_0 = \mathcal{N}([6, -3], I/2)$, $\mathbb{P}_1 = \mathcal{N}([6, 0], I/2)$, and $\mathbb{P}_2 = \mathcal{N}([6, 3], I/2)$ for the target graph. In both graphs, the intra-class edge probability is set to 0.1, while the inter-class edge probability is set to 0.02. To widen the distribution gap, we further modify the target graph by replacing 25% of the randomly generated intra-class edges with intra-class edges that connect the top-k dissimilar nodes based on their attributes.

Figure 6 demonstrates knowledge transfer in UDA-GCN, TDSS, Direct ST, and GGDA-GCN via the label assignments from training. While visualized in Ω_x for clarity, we must emphasize that the actual computations operate over $\Omega_x \times \Omega_a$ with interactions between self-information and neighbor information — where the key complexity arises. The figure reveals

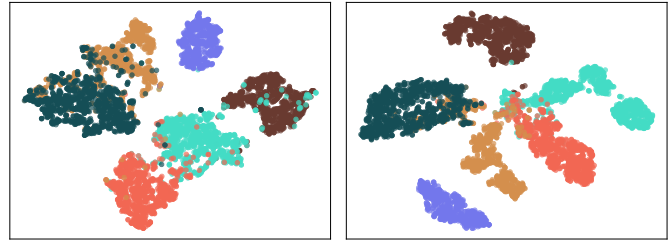


Fig. 5. Visualization of target graph node embeddings for the task A2 to D2, where distinct colors signify different class labels. The left side shows the result from UDA-GCN and the right side shows that from GGDA-GCN.

TABLE IV
COMPARISON OF RUNTIME ON ARXIV(07-18) (FOR 1000 EPOCHS) AND AVERAGE PERFORMANCE SCORE ACROSS ALL DATASETS.

Model	Runtime (seconds)	Avg. Score
SpecReg	532.3	63.9
A2GNN	643.6	66.8
ACDNE	1849.9 (for 200 epochs)	65.4
GraphAlign	1422.7 (for 200 epochs)	61.1
GGDA-GCN	668.2 (graph generation) + 208.5 (domain progression) = 876.7	72.9

that, through careful graph generation and iterative domain construction strategy, GGDA effectively creates an optimal domain path over the manifold. It regularizes transfer errors over consecutive domains, thus overcoming the significant distribution gap with minimal noise disturbance to allow smooth and accurate transition to the target graph.

Knowledge distortion occurs with methods other than GGDA-GCN. For DIR models (i.e., UDA-GCN and TDSS), domain alignment forcibly matches the overall distributions while neglecting source-target correlations in the joint space, rendering them unreliable under a widened distribution gap. As for Direct ST, pseudo-labels are initially assigned to target nodes solely based on the source model, but with large domain discrepancies, many become inaccurate. The erroneous information propagates upon the target graph during subsequent training stages, impeding proper learning.

H. Runtime Comparison

Table IV compares the model efficiency on transfer Arxiv(07-18), the largest dataset. All models are trained until convergence at either around 1000 or 200 epochs. Our GGDA framework achieves a runtime comparable to other models while significantly improving target predictions. Despite the non-generative nature of DIR models, they rely heavily on advanced encoder designs and regularizations, leading to costly computations such as eigendecomposition and topological matching. As for GraphAlign, a data-centric method, the graph generation is computationally intensive when the generated graph exceeds 1% of the target graph size, i.e., a huge trade-off between time and performance. Overall, our novel GGDA framework strikes an optimal balance via the accelerated graph generation technique and the careful domain constructions that attain minimal transfer information loss.

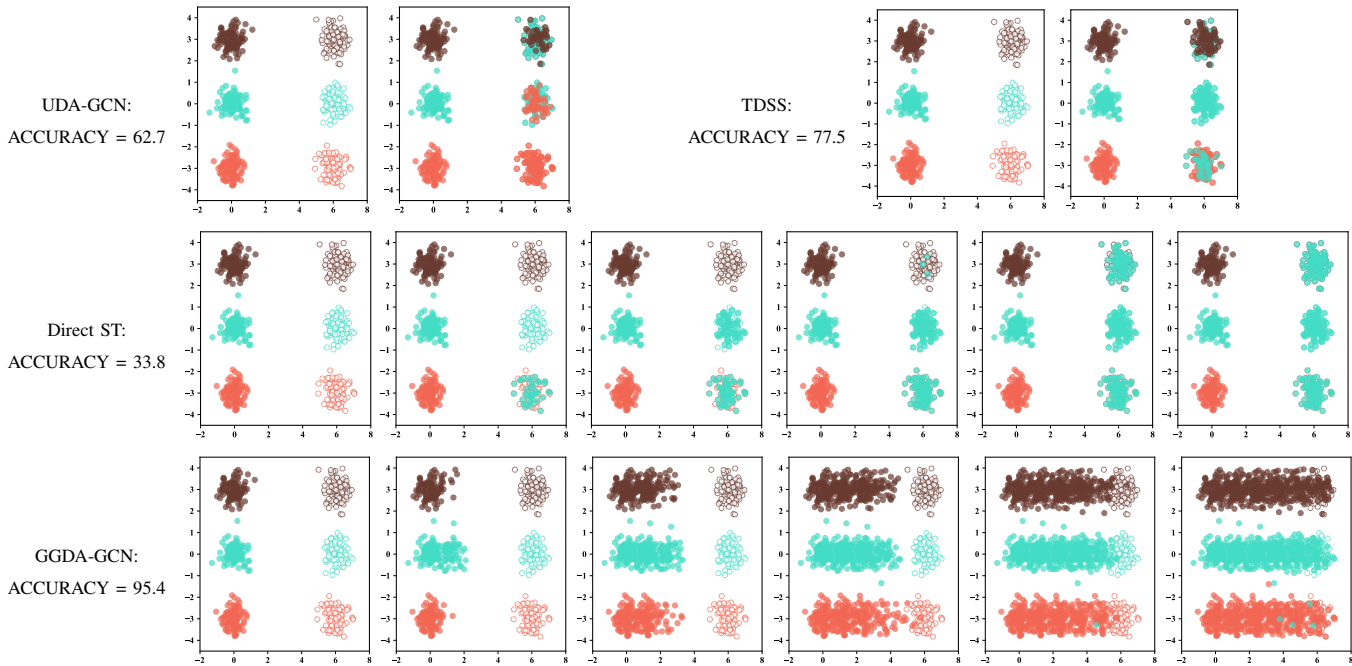


Fig. 6. Each plane represents a 2-dimensional space Ω_x (note that all computations are performed over the product space $\Omega_x \times \Omega_a$, i.e., with both features and structures on graph (non-IID), but the visualization is shown on Ω_x for clarity). Solid circles represent the ground-truth source labels or the assigned pseudo-labels (i.e., predictions) on each sample, whereas hollow circles represent the ground-truth target labels. Distinct colors indicate different classes. The assignments of labels throughout the training process are shown from left to right, with the leftmost planes showing the source and target labels before training. Specifically, UDA-GCN and TDSS employ single-stage training, while Direct ST and GGDA-GCN employ multi-stage training.

X. CONCLUSION

This work presents a pioneering effort to tackle a significant source-target graph discrepancy and to establish a graph gradual domain adaptation (GGDA) framework. We propose efficient FGW-based generation of knowledge-preserving intermediate graphs for bridging the gap, upon which we develop vertex-based domain constructions that approach the shortest adaptation path via information loss minimization. Our framework bounds the target generalization error by establishing implementable lower and upper bounds for $W_p(\mu_t, \mu_{t+1})$, an intractable metric in the graph context. Future work may explore GGDA extensions tailored to specific scenarios.

REFERENCES

- [1] S. J. Pan and Q. Yang, "A survey on transfer learning," *IEEE Transactions on knowledge and data engineering*, vol. 22, no. 10, pp. 1345–1359, 2009.
- [2] Y. Ganin, E. Ustinova, H. Ajakan, P. Germain, H. Larochelle, F. Laviolette, M. March, and V. Lempitsky, "Domain-adversarial training of neural networks," *Journal of machine learning research*, vol. 17, no. 59, pp. 1–35, 2016.
- [3] M.-Y. Liu and O. Tuzel, "Coupled generative adversarial networks," *Advances in neural information processing systems*, vol. 29, 2016.
- [4] K. Bousmalis, G. Trigeorgis, N. Silberman, D. Krishnan, and D. Erhan, "Domain separation networks," *Advances in neural information processing systems*, vol. 29, 2016.
- [5] M. Long, H. Zhu, J. Wang, and M. I. Jordan, "Deep transfer learning with joint adaptation networks," in *International conference on machine learning*. PMLR, 2017, pp. 2208–2217.
- [6] E. Tzeng, J. Hoffman, K. Saenko, and T. Darrell, "Adversarial discriminative domain adaptation," in *Proceedings of the IEEE conference on computer vision and pattern recognition*, 2017, pp. 7167–7176.
- [7] Y. Wu, E. Winston, D. Kaushik, and Z. Lipton, "Domain adaptation with asymmetrically-relaxed distribution alignment," in *International conference on machine learning*. PMLR, 2019, pp. 6872–6881.
- [8] A. Singh, "Clda: Contrastive learning for semi-supervised domain adaptation," *Advances in Neural Information Processing Systems*, vol. 34, pp. 5089–5101, 2021.
- [9] K. Shen, R. M. Jones, A. Kumar, S. M. Xie, J. Z. HaoChen, T. Ma, and P. Liang, "Connect, not collapse: Explaining contrastive learning for unsupervised domain adaptation," in *International conference on machine learning*. PMLR, 2022, pp. 19 847–19 878.
- [10] T. N. Kipf and M. Welling, "Semi-supervised classification with graph convolutional networks," *arXiv preprint arXiv:1609.02907*, 2016.
- [11] P. Veličković, G. Cucurull, A. Casanova, A. Romero, P. Lio, and Y. Bengio, "Graph attention networks," *arXiv preprint arXiv:1710.10903*, 2017.
- [12] W. Hamilton, Z. Ying, and J. Leskovec, "Inductive representation learning on large graphs," *Advances in neural information processing systems*, vol. 30, 2017.
- [13] K. Xu, W. Hu, J. Leskovec, and S. Jegelka, "How powerful are graph neural networks?" *arXiv preprint arXiv:1810.00826*, 2018.
- [14] M. Wu, S. Pan, C. Zhou, X. Chang, and X. Zhu, "Unsupervised domain adaptive graph convolutional networks," in *Proceedings of The Web Conference 2020*, 2020, pp. 1457–1467.
- [15] X. Zhang, Y. Du, R. Xie, and C. Wang, "Adversarial separation network for cross-network node classification," in *Proceedings of the 30th ACM international conference on information & knowledge management*, 2021, pp. 2618–2626.
- [16] Y. Mao, J. Sun, and D. Zhou, "Augmenting knowledge transfer across graphs," in *2022 IEEE International Conference on Data Mining (ICDM)*. IEEE, 2022, pp. 1101–1106.
- [17] S. Liu, T. Li, Y. Feng, N. Tran, H. Zhao, Q. Qiu, and P. Li, "Structural re-weighting improves graph domain adaptation," in *International Conference on Machine Learning*. PMLR, 2023, pp. 21 778–21 793.
- [18] J. Wu, J. He, and E. Ainsworth, "Non-iid transfer learning on graphs," in *Proceedings of the AAAI Conference on Artificial Intelligence*, vol. 37, no. 9, 2023, pp. 10 342–10 350.
- [19] M. Liu, Z. Fang, Z. Zhang, M. Gu, S. Zhou, X. Wang, and J. Bu, "Rethinking propagation for unsupervised graph domain adaptation," *arXiv preprint arXiv:2402.05660*, 2024.
- [20] Y. Wang, R. Zhu, P. Ji, and S. Li, "Open-set graph domain adaptation via separate domain alignment," in *Proceedings of the AAAI Conference on Artificial Intelligence*, vol. 38, no. 8, 2024, pp. 9142–9150.
- [21] X. Shen, Q. Dai, F.-I. Chung, W. Lu, and K.-S. Choi, "Adversarial deep network embedding for cross-network node classification," in

- Proceedings of the AAAI conference on artificial intelligence*, vol. 34, no. 03, 2020, pp. 2991–2999.
- [22] Q. Dai, X.-M. Wu, J. Xiao, X. Shen, and D. Wang, “Graph transfer learning via adversarial domain adaptation with graph convolution,” *IEEE Transactions on Knowledge and Data Engineering*, vol. 35, no. 5, pp. 4908–4922, 2022.
- [23] Y. You, T. Chen, Z. Wang, and Y. Shen, “Graph domain adaptation via theory-grounded spectral regularization,” in *The eleventh international conference on learning representations*, 2023.
- [24] H. Zhao, R. T. Des Combes, K. Zhang, and G. Gordon, “On learning invariant representations for domain adaptation,” in *International conference on machine learning*. PMLR, 2019, pp. 7523–7532.
- [25] B. Tan, Y. Zhang, S. Pan, and Q. Yang, “Distant domain transfer learning,” in *Proceedings of the AAAI conference on artificial intelligence*, vol. 31, no. 1, 2017.
- [26] J.-Y. Zhu, T. Park, P. Isola, and A. A. Efros, “Unpaired image-to-image translation using cycle-consistent adversarial networks,” in *Proceedings of the IEEE international conference on computer vision*, 2017, pp. 2223–2232.
- [27] H.-K. Hsu, C.-H. Yao, Y.-H. Tsai, W.-C. Hung, H.-Y. Tseng, M. Singh, and M.-H. Yang, “Progressive domain adaptation for object detection,” in *Proceedings of the IEEE/CVF winter conference on applications of computer vision*, 2020, pp. 749–757.
- [28] M. Xu, J. Zhang, B. Ni, T. Li, C. Wang, Q. Tian, and W. Zhang, “Adversarial domain adaptation with domain mixup,” in *Proceedings of the AAAI conference on artificial intelligence*, vol. 34, no. 04, 2020, pp. 6502–6509.
- [29] J. Na, H. Jung, H. J. Chang, and W. Hwang, “Fixbi: Bridging domain spaces for unsupervised domain adaptation,” in *Proceedings of the IEEE/CVF conference on computer vision and pattern recognition*, 2021, pp. 1094–1103.
- [30] A. Kumar, T. Ma, and P. Liang, “Understanding self-training for gradual domain adaptation,” in *International conference on machine learning*. PMLR, 2020, pp. 5468–5479.
- [31] S. Abnar, R. v. d. Berg, G. Ghiasi, M. Dehghani, N. Kalchbrenner, and H. Sedghi, “Gradual domain adaptation in the wild: When intermediate distributions are absent,” *arXiv preprint arXiv:2106.06080*, 2021.
- [32] H.-Y. Chen and W.-L. Chao, “Gradual domain adaptation without indexed intermediate domains,” *Advances in neural information processing systems*, vol. 34, pp. 8201–8214, 2021.
- [33] H. Wang, B. Li, and H. Zhao, “Understanding gradual domain adaptation: Improved analysis, optimal path and beyond,” in *International Conference on Machine Learning*. PMLR, 2022, pp. 22784–22801.
- [34] S. Sagawa and H. Hino, “Gradual domain adaptation via normalizing flows,” *arXiv preprint arXiv:2206.11492*, 2022.
- [35] Y. He, H. Wang, B. Li, and H. Zhao, “Gradual domain adaptation: Theory and algorithms,” *arXiv preprint arXiv:2310.13852*, 2023.
- [36] V. Titouan, N. Courty, R. Tavenard, and R. Flamary, “Optimal transport for structured data with application on graphs,” in *International Conference on Machine Learning*. PMLR, 2019, pp. 6275–6284.
- [37] Y. Zhang, G. Song, L. Du, S. Yang, and Y. Jin, “Dane: Domain adaptive network embedding,” *arXiv preprint arXiv:1906.00684*, 2019.
- [38] G. Guo, C. Wang, B. Yan, Y. Lou, H. Feng, J. Zhu, J. Chen, F. He, and S. Y. Philip, “Learning adaptive node embeddings across graphs,” *IEEE Transactions on Knowledge and Data Engineering*, vol. 35, no. 6, pp. 6028–6042, 2022.
- [39] M. Wu, S. Pan, and X. Zhu, “Attraction and repulsion: Unsupervised domain adaptive graph contrastive learning network,” *IEEE Transactions on Emerging Topics in Computational Intelligence*, vol. 6, no. 5, pp. 1079–1091, 2022.
- [40] Z. Qiao, X. Luo, M. Xiao, H. Dong, Y. Zhou, and H. Xiong, “Semi-supervised domain adaptation in graph transfer learning,” *arXiv preprint arXiv:2309.10773*, 2023.
- [41] B. Shi, Y. Wang, F. Guo, J. Shao, H. Shen, and X. Cheng, “Improving graph domain adaptation with network hierarchy,” in *Proceedings of the 32nd ACM International Conference on Information and Knowledge Management*, 2023, pp. 2249–2258.
- [42] R. Cai, F. Wu, Z. Li, P. Wei, L. Yi, and K. Zhang, “Graph domain adaptation: A generative view,” *ACM Transactions on Knowledge Discovery from Data*, vol. 18, no. 3, pp. 1–24, 2024.
- [43] S. Liu, D. Zou, H. Zhao, and P. Li, “Pairwise alignment improves graph domain adaptation,” *arXiv preprint arXiv:2403.01092*, 2024.
- [44] Q. Zhu, C. Yang, Y. Xu, H. Wang, C. Zhang, and J. Han, “Transfer learning of graph neural networks with ego-graph information maximization,” *Advances in Neural Information Processing Systems*, vol. 34, pp. 1766–1779, 2021.
- [45] R. Huang, J. Xu, X. Jiang, R. An, and Y. Yang, “Can modifying data address graph domain adaptation?” in *Proceedings of the 30th ACM SIGKDD Conference on Knowledge Discovery and Data Mining*, 2024, pp. 1131–1142.
- [46] N. Yin, L. Shen, B. Li, M. Wang, X. Luo, C. Chen, Z. Luo, and X.-S. Hua, “Deal: An unsupervised domain adaptive framework for graph-level classification,” in *Proceedings of the 30th ACM International Conference on Multimedia*, 2022, pp. 3470–3479.
- [47] N. Yin, L. Shen, M. Wang, L. Lan, Z. Ma, C. Chen, X.-S. Hua, and X. Luo, “Coco: A coupled contrastive framework for unsupervised domain adaptive graph classification,” in *International Conference on Machine Learning*. PMLR, 2023, pp. 40040–40053.
- [48] B. Gong, Y. Shi, F. Sha, and K. Grauman, “Geodesic flow kernel for unsupervised domain adaptation,” in *2012 IEEE conference on computer vision and pattern recognition*. IEEE, 2012, pp. 2066–2073.
- [49] R. Gopalan, R. Li, and R. Chellappa, “Domain adaptation for object recognition: An unsupervised approach,” in *2011 international conference on computer vision*. IEEE, 2011, pp. 999–1006.
- [50] G. Peyré, M. Cuturi *et al.*, “Computational optimal transport: With applications to data science,” *Foundations and Trends® in Machine Learning*, vol. 11, no. 5-6, pp. 355–607, 2019.
- [51] R. Gong, W. Li, Y. Chen, and L. V. Gool, “Dlow: Domain flow for adaptation and generalization,” in *Proceedings of the IEEE/CVF conference on computer vision and pattern recognition*, 2019, pp. 2477–2486.
- [52] L. Shi and W. Liu, “Adversarial self-training improves robustness and generalization for gradual domain adaptation,” *Advances in Neural Information Processing Systems*, vol. 36, 2024.
- [53] H. Shimodaira, “Improving predictive inference under covariate shift by weighting the log-likelihood function,” *Journal of statistical planning and inference*, vol. 90, no. 2, pp. 227–244, 2000.
- [54] V. Garg, S. Jegelka, and T. Jaakkola, “Generalization and representational limits of graph neural networks,” in *International Conference on Machine Learning*. PMLR, 2020, pp. 3419–3430.
- [55] T. Vayer, L. Chapel, R. Flamary, R. Tavenard, and N. Courty, “Fused gromov-wasserstein distance for structured objects,” *Algorithms*, vol. 13, no. 9, p. 212, 2020.
- [56] G. Karypis and V. Kumar, “A fast and high quality multilevel scheme for partitioning irregular graphs,” *SIAM Journal on scientific Computing*, vol. 20, no. 1, pp. 359–392, 1998.
- [57] M. Zhu, X. Wang, C. Shi, H. Ji, and P. Cui, “Interpreting and unifying graph neural networks with an optimization framework,” in *Proceedings of the Web Conference 2021*, 2021, pp. 1215–1226.
- [58] C. Druţu and M. Kapovich, *Geometric group theory*. American Mathematical Soc., 2018, vol. 63.
- [59] J. Li, X. Hu, J. Tang, and H. Liu, “Unsupervised streaming feature selection in social media,” in *Proceedings of the 24th ACM International Conference on Information and Knowledge Management*, 2015, pp. 1041–1050.
- [60] W. Hu, M. Fey, M. Zitnik, Y. Dong, H. Ren, B. Liu, M. Catasta, and J. Leskovec, “Open graph benchmark: Datasets for machine learning on graphs,” *Advances in neural information processing systems*, vol. 33, pp. 22118–22133, 2020.
- [61] P. Sen, G. Namata, M. Bilgic, L. Getoor, B. Galligher, and T. Eliassi-Rad, “Collective classification in network data,” *AI magazine*, vol. 29, no. 3, pp. 93–93, 2008.
- [62] B. Rozemberczki, C. Allen, and R. Sarkar, “Multi-scale attributed node embedding,” *Journal of Complex Networks*, vol. 9, no. 2, p. cnab014, 2021.
- [63] M. Long, Z. Cao, J. Wang, and M. I. Jordan, “Conditional adversarial domain adaptation,” *Advances in neural information processing systems*, vol. 31, 2018.
- [64] Y. Zhang, T. Liu, M. Long, and M. Jordan, “Bridging theory and algorithm for domain adaptation,” in *International conference on machine learning*. PMLR, 2019, pp. 7404–7413.
- [65] W. Chen, G. Ye, Y. Wang, Z. Zhang, L. Zhang, D. Wang, Z. Zhang, and F. Zhuang, “Smoothness really matters: A simple yet effective approach for unsupervised graph domain adaptation,” in *Proceedings of the AAAI Conference on Artificial Intelligence*, vol. 39, no. 15, 2025, pp. 15875–15883.
- [66] L. Van der Maaten and G. Hinton, “Visualizing data using t-sne,” *Journal of machine learning research*, vol. 9, no. 11, 2008.
- [67] Y. Deshpande, S. Sen, A. Montanari, and E. Mossel, “Contextual stochastic block models,” *Advances in Neural Information Processing Systems*, vol. 31, 2018.